Heriot-Watt University
Research Gateway

On the Development of a 7-DoF SPP Robotic Arm

Citation for published version:
Haider, AFA, Al-Qrimli, HFA & Kumar, TN 2011, 'On the Development of a 7-DoF SPP Robotic Arm', Paper presented at SICE Annual Conference 2011, Tokyo, Japan, 13/09/11 - 18/09/11 pp. 930-934.

Link:
Link to publication record in Heriot-Watt Research Portal

Document Version:
Peer reviewed version

General rights
Copyright for the publications made accessible via Heriot-Watt Research Portal is retained by the author(s) and / or other copyright owners and it is a condition of accessing these publications that users recognise and abide by the legal requirements associated with these rights.

Take down policy
Heriot-Watt University has made every reasonable effort to ensure that the content in Heriot-Watt Research Portal complies with UK legislation. If you believe that the public display of this file breaches copyright please contact open.access@hw.ac.uk providing details, and we will remove access to the work immediately and investigate your claim.

Download date: 11. Dec. 2024

SICE Annual Conference 2011
September 13-18, 2011, Waseda University, Tokyo, Japan

On the Development of a 7-DoF SPP Robotic Arm

Haider A. F. Almurib, Haidar Fadhil Al-Qrimli, and T. Nandha Kumar

Department of Electrical & Electronic Engineering, The University of Nottingham Malaysia Campus
Jalan Broga, 43500 Semenyih, Malaysia
(Tel : +60-3-8924-8613; E-mail: haider.abbas@nottingham.edu.my)

Abstract: This paper describes the mechanical design, analysis, and prototyping of a 7 DoF robotic arm that uses electrical actuators as its muscles. The structure of the arm is a hybrid Serial-Parallel-Parallel (SPP) configuration. The robotic arm is similar in size and structure to the human arm and can imitate the human arm movements; the 3 DoF shoulder has a serial link configuration; the 1 DoF elbow is a parallel configuration; and the 3 DoF wrist has a parallel configuration. Finite element analysis of critical components are also carried out.

Keywords: Robotic arm, forward kinematics, serial and parallel configurations, workspace.

1. INTRODUCTION

Robotic arm has been referred to as industrial manipulator and characters emulated manipulators of a human arm are called articulated arms, which joints are all rotary. Motion of the human arm differs from the motion of articulated robot arms. Although the robot joints have fewer degrees of freedom, they are able to move with larger angles. For example, the elbow of an articulated robot can bend up or down, whereas a person can only bend their elbow in one direction with respect to the straight-arm position [1,2].

Many researchers have studied parallel manipulators intensely. That is because they found many advantages comparing to serial manipulators they have a high payload to the weight ratio, accurate and have simple and high structure rigidity, in addition the inverse kinematic problem has simple solution [3,4]. However, there are disadvantages as well for these types of manipulators similar to every other mechanism, smaller workspace; less dexterity and more complex kinematic and dynamic models are problems that parallel manipulators have as compared to serial manipulators. Parallel manipulators are very popular in many industrial applications, and there is a lot of DoF depend on the required no of degree of freedom [5-9].

In addition, there are many applications that we can find robotics now days, for example, in the rehabilitation field, there are specialized in robots for training the patients for recovery and for surgery [10,11]. There are many robotics arms; perhaps the PUMA is the most popular arm that has 6 degree of freedom. However, the control architecture is closed, the cost is high, and the controllers are large comparing to a small size of the arm. We can find other robotic arms that have low cost and size such as KATANA, but it has 5DOF and low payload [12,13].

In this paper, we focus on the design of the robotic arm, and workspace of the entire robotic arm including the upper arm (shoulder), forearm (elbow) and wrist. Electric motors used to actuate the arm; they are very effective as robot actuators but are also heavy devices.

2. ARM STRUCTURE

The mechanical design of the proposed robotic arm is illustrated in Fig. 1. The second section of the paper will describe and explain the rationale behind such a design.

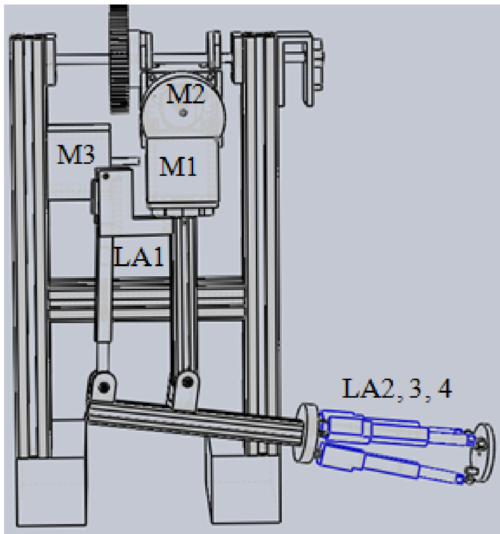

Fig.1 Main structure.

2.1 Actuation

The actuators used in this design are electrical actuators; three rotary motors in the shoulder and four linear motors, one in the elbow and three in the wrist that can enable 360° rotation. The motors were chosen based on their maximum torque, weight and dimension to suit the design of the robotic arm. Another hardware used to complete the design is motor drivers, rotary encoders and the microcontroller. The shoulder motor (M2) is selected to be a stepping motor that should provide a high torque of 8N.m and it rotates along the axis out of the page. The other shoulder motors (M1 and M3) both use the same type of motor that is a stepper motor and provide 1.28N.m. A pulley system is employed to increase the torque of the (M3) shoulder motor. The pulley system selected for this application is

 PR0001/11/0000-0930 ¥400 © 2011 SICE

timing belt that has 1:4 gear ratio. The linear actuator designed for the elbow should withstand 45N force while the 3 linear actuators at the wrist are selected to bear 12N. In Fig. 1, M refers to a rotary motor while LA refers to liner actuator.

2.2 Torque requirements

The design was first approached by obtaining the mechanical design of the robotic arm. Initially, parameters were set so that the engineering calculations could be performed to justify the design of the robotic arm. The length and the degree of freedom of the robotic arm to be analogous to that of a typical human arm. For each of these motions, a motor required so the torque required to be calculated to rotate the robotic arm at each joint. As illustrated in Fig. 1 the rotary motors are denoted as by M1, M2, and M3 respectively, whereas the linear actuator is denoted as LA1. The maximum torque occurs when motor M1 rotates the lower links (L2, L1 and wrist) 90º from its initial position. The maximum torque on M1 occurs when the lower link is parallel to the perpendicular distance from the point of the acting force. The torques are better calculated from the illustration in Fig. 2.

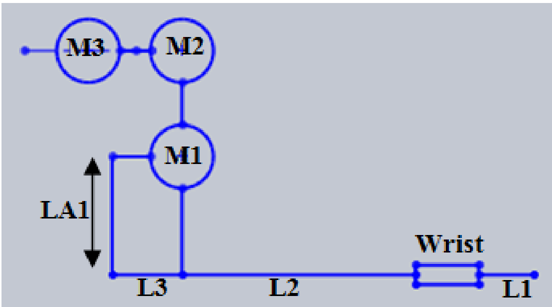

Fig. 2. Coordinate system of the arm.

The torque of M1 (T1) = (mass at end of link L1 * lower link length) + [(1/2 (L1) + L2W) * mass of L1] + [mass of wrist * L2W] + [1/2 * L2W * mass of link L2W], the value of T1 will be (1.96Nm). Since L3 and LA1 are behind motor M1 at all angle of rotations, this enables the mass of LA1 to produce a torque that opposes the torque produced by the lower link, thus effectively reducing the actual torque needed by motor M1. This is illustrated in Fig. 3.

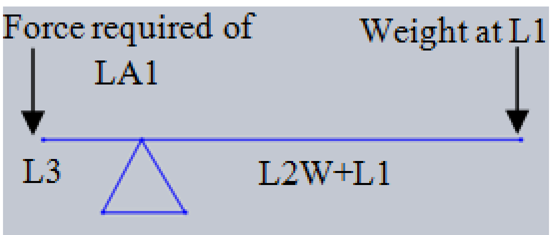

Fig. 3. Forces applied on the arm.

Torque produced the linear actuator LA1 at 50mm distance (TLA1) = [mass of LA1*L3]. Therefore, the actual torque needed by M1 to withstand the maximum possible applied torque on the lower link is $T_{actual} = T_1 - T_{LA1}$.

The amount of torque required on M2 and M3, considering the center point of rotation on M2 will be at maximum when the entire robotic arm is stretched out horizontally. Length 3 (L3) is neglected as it carries no influence to the torque needed at motor M2. The equation to calculate M2 torque:

T_2= [mass of L1* (L1+ L2W+L4)] + [(1/2 (L1) + L2W + L4) * mass of L1] + [mass of wrist * (l2w+l4)] + [(1/2 (L2W) + L4) * mass L2W] + [mass of M1 + L4] + [1/2(L4) *mass of L4]

Since linear actuators translate in a linear motion, its selection can't be based on the torque parameter, rather, a force measurement is used. The linear actuator LA1 will require a pushing force higher or equivalent to the mass of the entire lower link to support and move the link up and down. In other words, the force produced by LA1 over the L3 must be able to balance the weight at the end of the L1 over the length L1+L2W and it's simplified in Fig. 3. The force required (FLA1) calculated based upon the principle of balance of equally distributed forces, (FLA1* L3= Weight at L1 * L2W+L1). The force requires of each linear actuator at the wrist, FLA2, FLA3. FLA4 are identical and considerably small. Using the same techique as the FLA1 (principle of force balancing), and assuming the fulcrum to be located at the middle of L1. The total force required of the wrist will have to be divided by 3 (for 3 linear actuators). Table 1 shows a summary on the calculated torque required for each motor and Table 2 shows the force required for each linear actuator.

Table 1: Torque required for each motor

Motor	Torque required (Nm)
M1	1.94
M2	5.18
M3	5.18

Table 2: Force required for each linear actuator

Linear actuator	Force required (N)
LA1	29.4
LA2	1.6
LA3	1.6
LA4	1.6

2.3 Materials and machines

The main structure of the robotic arm is constructed using aluminum. Aluminum profile serves as the bone frame of the arm. It has a high mechanical strength and will be able to withstand the mechanical forces enforced on the robotic arm, light in weight and have a cheap price, Aluminum plates was used as joints and connections. Ball bearings and ball and socket joints were used in the structure of the robotic arm. Table 3 shows the mechanical properties of the material used.

Table 3: Material properties

Property	Value	Units
Aluminum Profile		
Elastic Modulus	6.9e+010	N/m^2
Poisons Ratio	0.33	
Shear Modulus	2.58e+010	N/m^2
Mass Density	2700	kg/m^3
Tensile Strength	185000000	N/m^3
Yield Strength	145000000	N/m^2
Aluminum Plates		
Elastic Modulus	6.900000067e+010	N/m^2
Poisons Ratio	0.33	
Shear Modulus	2.600000013e+010	N/m^2
Mass Density	2700	kg/m^3
Tensile Strength	239999999.6	N/m^3
Yield Strength	227526990.7	N/m^2

3. FEA SIMULATIONS

We present here a three dimensional FE model of the shoulder shaft that is holding the entire arm and the forearm (elbow joints). SolidWorks software was used to make the modeling and the FEA. The model's geometry is solid we defined the dimensions, volume and mass for each part, number of nodes and element was selected as well. The material selected is aluminum the mechanical properties were shown in Table 3. Static structural analysis was done on the parts. Different dimensions have been tested for the parts and from the analysis the best suitable dimensions have been chosen to the robotic arm.

Fig. 4 shows the CAD model and the mesh of the shaft. Displacement, factor of safety (FOS) and von misses analysis had been carried out. The displacement analysis had been carried to check the deformation of the shaft when a certain load is given while von misses analysis had been carried out to check the maximum stress on the shaft. The shaft considers being the most critical part in the arm because it holds all the arm structure and the belt tension 120N.

As shown the maximum displacement is 0.00017 mm, which is very small. So using the shaft made of aluminum is perfect with 6kg weight, which is under control. Using aluminum is cheaper and lighter in weight comparing to steel. The maximum stress as shown in Fig. 12 is 74.9553MPa which is lower than the yield stress of the aluminum. Safety factor is the structural strength divided by the minimum structural strength required. The greater the safety factor, the more stress cycles the structure can take. For design purposes, a safety factor (ratio of yield stress by normal stress) bigger than 3 is taken into account.

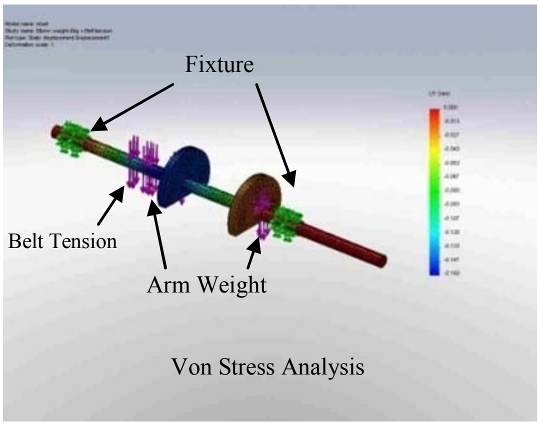

Fig. 4. Shaft-arm weight and belt tension analysis.

Fig. 5 shows the elbow joint's analysis. The entire arm subjected to 3kg, which is the maximum load that the arm can hold the maximum von mises to be 75.85MPa. For the maximum displacement found to be 0.11852mm which is considered extremely small and can be ignored and in zero scaling this deformation can’t be observed. The safety factor value of the mechanism is 4.9 that mean that the design is safe.

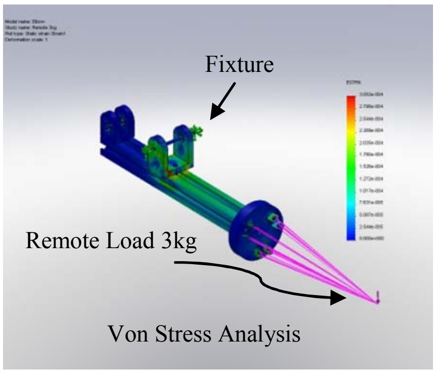

Fig. 5. Elbow analysis.

One of the critical parts that we need to make analysis on is the linear motor holder that has been made from aluminum alloy. It is fixed on the central link of the arm by using a set of screws. As shown in Fig. 6, the maximum von Mises Stress value is (46.9256 Mpa) the maximum deformation that occurs is (0.0740356 mm).

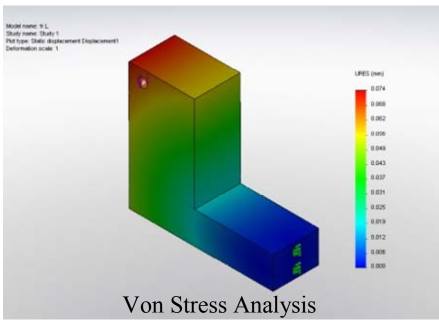

Fig. 6. Elbow motor holder analysis.

Fig. 7 it shows the wrist analysis. The maximum von Mises Stress value is 9.7143 Mpa. The maximum deformation that occurs on the wrist is 0.0015349 mm. The values of the von Mises Stress are less than the yielding point of the material, and the deformation occurs is very small that led us to say that the analysis of the critical robotic arm parts consider safe so the design is successful.

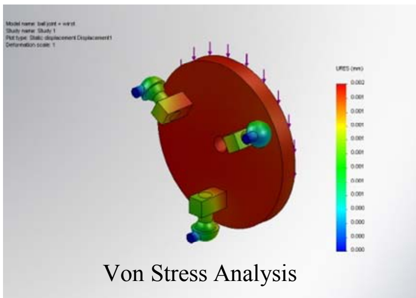

Fig. 7. Ball joint and wrist analysis.

4. KINEMATICS AND WORKSPACE

Fig. 8 illustrates the frames of the robotic arm. The DH parameters are calculated and given in Table 4, to make a relationship between the individual joints of the manipulator and the position and orientation of the end-effector. Frame $\{X_0Y_0Z_0\}$ is fixed to the base of the shoulder. As can be seen from the figure, frame $\{X_1Y_1Z_1\}$ and $\{X_2Y_2Z_2\}$ is attached to the end point of the shoulder. Similarly frame $\{X_3Y_3Z_3\}$ is attached to the elbow moved with the joint distance. Frame $\{X_4Y_4Z_4\}$ is attached to the end point of the hand.

The results of applying the DH process is shown in Eq. (1) where $c_i = cos(\theta_i)$ *and* $s_i = sin(\theta_i)$.

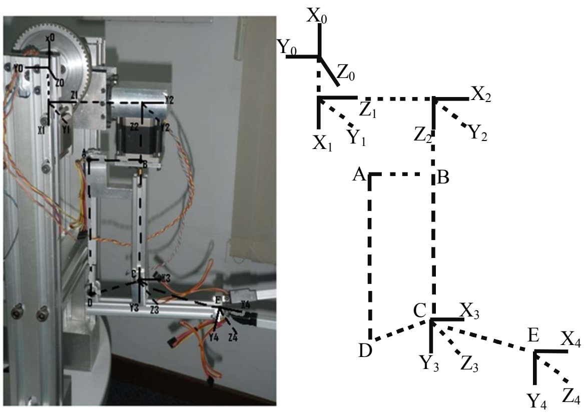

Fig 8. Coordinate system of the arm

Table 4: Denavit-Hartenberg parameters of the arm.

Link (Joint) *i*	d_i	a_i	α_i	θ_i
1	0	a_1	-90°	θ_1
2	d_1	0	90°	θ_2
3	d_3	0	90^0	θ_3
4	0	a_4	0	θ_4

Mechanical limitations such as location of the joints, joint angle limits and the manipulator size affect the workspace of the arm. The workspace of the assembly of the upper arm and forearm is a volume. It's a space between two and three dimensional spherical surfaces. MATLAB programming software was used to calculate the workspace of the model and the results of the simulation is shown in Fig. 9 and 10 for the 3D space and 2D spaces, respectively. The joints limits used in the workspace simulation are shown in Table 5.

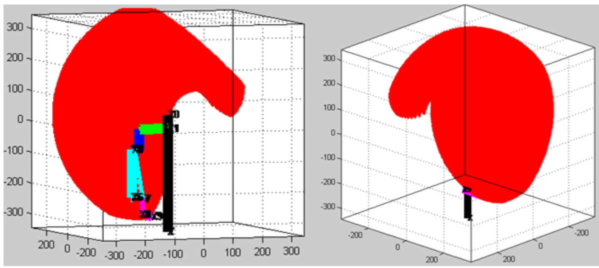

Fig. 9. Workspace of the 7-DOF robotic arm.

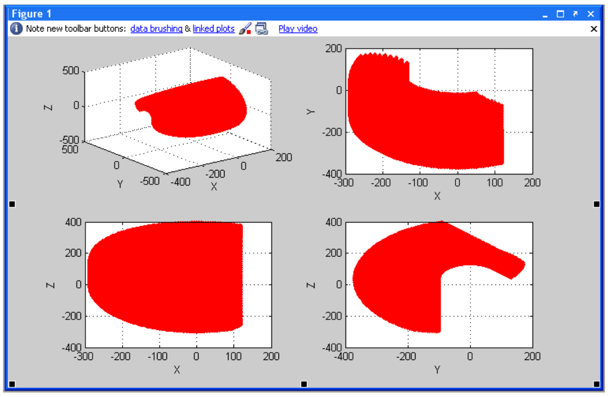

Fig. 10. Workspace of the 7-DOF robotic arm in 2D.

Table 5: Joints limits of the 7-DOF robotic arm

Limits	Range
Joint 1	$-\pi < \theta_1 < -\pi/4$
Joint 2	$0 < \theta_2 < 3\pi/4$
Joint 3	$0 < \theta_3 < -\pi/4$
Actuator	$165 < L_{AD} < 230$

$$
{}^0T_4 = \begin{bmatrix} c_1c_2c_3c_4 - s_1s_3c_4 + c_1s_2s_4 & -c_1c_2c_3s_4 + s_1s_3s_4 + c_1s_2c_4 & c_1c_2s_3 + s_1c_3 & a_4c_4(c_1c_2c_3 - s_1s_3) + a_4s_4c_1s_2 + d_3c_1s_2 - s_1d_2 + a_1c_1 \\ s_1c_2c_3c_4 + c_1s_3c_4 + s_1s_2s_4 & -s_1c_2c_3s_4 - c_1s_3s_4 + s_1s_2c_4 & s_1c_2s_3 - c_1c_3 & a_4c_4(s_1c_2c_3 + c_1s_3) + a_4s_4s_1s_2 + d_3s_1s_2 + c_1d_2 + a_1s_1 \\ -s_2c_3c_4 + c_2s_4 & s_2c_3s_4 + c_2c_4 & -s_2s_3 & -a_4c_4s_2c_3 + a_4s_4c_2 + d_3c_2 \\ 0 & 0 & 0 & 1 \end{bmatrix} \quad (1)
$$

5. CONCLUSION

The paper described the design of a robotic arm that has 7-DoF that targets mimicing the movements of human beings. The upper arm (shoulder) has 3-DoF and 1-DoF in the elbow. The wrist has 3-DoF. The upper arm has serial link configuration. The elbow has a parallel configuration and use liner actuator to duplicate the axial motion of the human arm. The same configuration is used for the wrist (parallel). The dimensions of the robotic arm are almost the same to average human being arms, and the workspace is acceptable. The dimensions of the robotic arm parts were based on finite element analysis of several dimensions. It was found that the Von Mises stress analysis subjected on the arm parts were below the maximum yield strength of the material used. The maximum deformation of the parts is negligible as they all deform in extremely small values and it's less than the value of the elasticity of the material.

AKNOWLEDGMENT

The researchers wish to thank the Ministry of Science, Technology and Innovation (MOSTI) Malaysia for funding this work through e-Science Fund Project No. 06-02-12-SF0072.

REFERENCES

[1] Joel C. Perry, Jacob Rosen, Design of a 7 Degree-of-Freedom Upper-Limb Powered Exoskeleton, BioRob 2006- The first IEEE / RAS-EMBS International Conference on Biomedical Robotics and Biomechatronics Pisa, Tuscany, Italy, February 20-22, 2006.

[2] Andre Schiele, Fundamentals of Ergonomic Exoskeleton Robots, ISBN: 978-90-8559-379-9, 2008.

[3] Iman Ebrahimi, Juan A. Carretero, Roger Boudreau, 3-PRRR redundant planar parallel manipulator: Inverse displacement, workspace and singularity analyses, Mechanism and Machine Theory, Volume 42, Issue 8, Pages 1007-1016, 2007.

[4] Peter B. Goldsmith, Design and Kinematics of a Three-Legged Parallel Manipulator, IEEE TRANSACTIONS ON ROBOTICS AND AUTOMATION, VOL. 19, NO. 4, 2003.

[5] Chao Daihong, Zong Guanghua, and Liu Rong, Design of a 6-DOF Compliant Manipulator Based on Serial-Parallel Architecture, Proceedings of the 2005 IEEE/ASME International Conference on Advanced Intelligent Mechatronics Monterey, California, USA, 2005.

[6] Hagay Bamberger and Moshe Shoham, A Novel Six Degrees-of Freedom Parallel Robot for MEMS Fabrication, IEEE Transactions On Robotics, Vol. 23, NO. 2, 2007.

[7] H. Pendar, M. Vakil, R. Fotouhi and H. Zohoor, Kinematic Analysis of the Spherically Actuated Platform Manipulator, IEEE International Conference on Robotics and Automation Roma, Italy, 10-14, 2007.

[8] Chifu Yang, Jingfeng He Hongzhou Jiang Junwei Han, Modeling and Simulation of 6-DOF Parallel Manipulator Based on PID Control with Gravity Compensation in Simulink/ADAMS, International Workshop on Modelling, Simulation and Optimization, 978-0-7695-3484, 2008.

[9] A. Mahmoodi, M. Aminzadeh, M.B. Menhaj and M. SabzehParvar, A Generalized Method for Determining Load Workspace of Spatial Parallel Mechanisms, 8th IEEE International Conference on Control and Automation Xiamen, China, June 9-11, 2010.

[10] Kazuo Tanie, Humanoid Robot and its Application Possibility, IEEE Conference on Multisensor Fusion and Integration for Intelligent Systems, 2003.

[11] Michael J. M, MD, (minimally invasive and robotic surgery), the journal of the American medical association, vol.285 no.5, .568-572, 2001.

[12] Mdnuel Lopes, Ricardo Beira, Miguel Prdsa, Jose Santos-Vlctor, An anthropomorphic robot torso for imitation: design and experiments, Proceedings of 2004 IEEEIRSJ International Conference on Intelligent Robots and Systems, Sendai, Japan, 2004.

[13] Katana Web Site, Neuronics intelligent and personal robotics, "www.neuronics.ch"